

## SIMULATION AND MEASUREMENTS FOR THE SUBSTANCE IDENTIFICATION BY AFM

Sylwia BABICZ<sup>1</sup>, Artur ZIELIŃSKI<sup>2</sup>

1. Gdańsk University of Technology, Faculty of Electronics, Telecommunications and Informatics,  
Department of Optoelectronics and Electronic Systems  
tel: +58 3486095                      fax: +58 3416132                      e-mail: sylwia.babicz@eti.pg.gda.pl
2. Gdańsk University of Technology, Chemical Faculty,  
Department of Electrochemistry, Corrosion and Materials Engineering  
tel: +58 3471440                      fax: +58 3471092                      e-mail: ziela@chem.pg.gda.pl

**Abstract:** Due to nanotechnology development, there is a strong pressure on research in nanoscale in various environments. An Atomic Force Microscope (AFM) allows to investigate topography of the sample and give some information about it's chemical composition. During the last two decades, the number of possible applications of AFM increased considerably. The AFM investigates the forces between the applied tip and the sample atoms. These forces are described by Lennard-Jones function. The paper presents a theoretical framework that explains a use of the AFM and presents the recorded signals, applied for substance characterization. Moreover, the preliminary results of the quartz surface measurements are enclosed. The presented way of the collected data analysis shows how to get parameters of the Lennard-Jones function, characteristic for the investigated sample.

**Keywords:** atomic force microscopy, chemicals identification, Leonard-Jones function

### 1. INTRODUCTION

The fast development of physics and electronics forced a creation of new microscopic devices which enable investigation of very small objects. Such investigation are important for technology improvements and quality of various objects, e.g. ZnO varistors [1].

The first tool for morphological analysis of the samples was the Scanning Tunneling Microscope (STM), which bases on the tunneling current flowing through the sample. This kind of research does not allow analysis of the samples having high resistivity (e.g. isolators). The AFM enables an examination of different materials (e.g. conductors or isolators) [2]. That is why the AFM was applied in quality control in optical industrial materials, semiconductor and magnetic storage media, and in crystalline sample structure analysis in chemistry and physics studies.

The AFM operates on the force acting between successive and repulsive atoms of the sample, placed on the piezoelectric tube, and the atoms of the scanning tip, placed at the free end of a cantilever [3]. Every surface depressions and bulges indicate changes of the cantilever

deflection. Typically, the deflection is measured using a laser spot reflected from the top surface of the cantilever into an array of photodiodes (Fig. 1). The forces are described by the Lennard-Jones function (Fig. 2), which determines the strength between the atoms of the studied sample and vibrating tip [4]:

$$F(s) = \frac{A_H R}{6\sigma^2} \left( \frac{\sigma^2}{s^2} - \frac{\sigma^8}{30s^8} \right) \quad (1)$$

where:  $\sigma$  – typical interatomic distance,  $A_H$  – Hamaker constant,  $R$  – tip radius,  $s$  – tip-sample distance

The Lennard-Jones function can also be described by a depth  $\varepsilon$  of the potential well:

$$F(s) = \frac{24\varepsilon}{\sigma} \left( \frac{2\sigma^{13}}{s^{13}} - \frac{\sigma^7}{s^7} \right) \quad (2)$$

where:  $\sigma$  – typical interatomic distance,  $\varepsilon$  – depth of the potential well,  $s$  – tip-sample distance

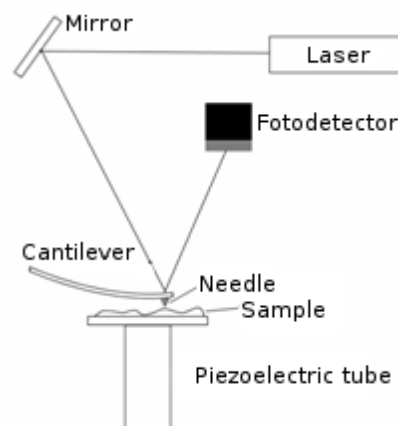


Fig. 1. Schematic illustration of the AFM device

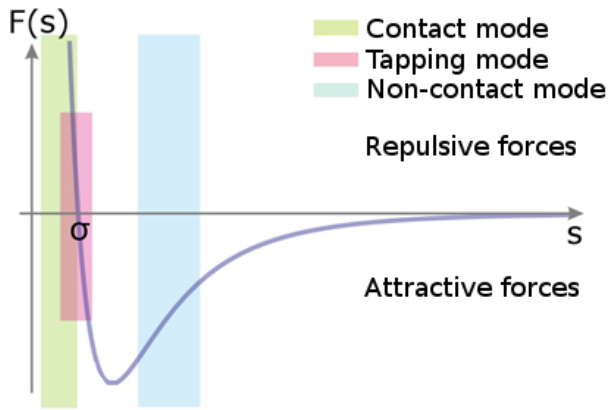


Fig. 2. Leonard-Jones force function with marked  $\sigma$ ,  $\epsilon$  and three typical modes

In the non-contact mode [5], the cantilever is stimulated by a sinusoidal voltage and oscillates over the sample's surface. As a result of interaction between the sample's and the needle's atoms the cantilever's oscillations are not identical with the stimulating signal. The Lennard-Jones function for non-contact mode is almost linear, so that we can expect that the response of the system will be close to a sine function.

Thus, the study of the stimulus signal and the response signal can determine parameters of the Lennard-Jones function and characterize the investigated sample.

## 2. SIMULATION

In order to assess different approaches to recover the Lennard-Jones function based on the described measurements, an input and an output signals were modeled. As a base, the function with the following parameters was used (Fig. 3):

$$\begin{aligned} A_H &= 0.425 \cdot 10^{-18} [J] \\ R &= 10 \cdot 10^{-9} [m] \\ f &= 17.97 \cdot 10^3 [Hz] \\ \sigma &= 0.35 \cdot 10^{-9} [m] \end{aligned} \quad (3)$$

where:  $A_H$  – Hamaker's constant for designed system,  $R$  – tip radius,  $f$  – resonance frequency of scanning tip,  $\sigma$  – typical interatomic distance [4]

As the next step, the position within the Lennard-Jones function at non-contact mode was selected. Then, it is necessary to select small fragment of the Lennard-Jones function in the non-contact mode, in which our tip is oscillating (Fig. 4). The range should be small and belong to the non-contact mode. In (4) are presented the assumed parameters of the stimulating signal:

$$\begin{aligned} Amp &= 0.5 \cdot 10^{-9} [J] \\ F_0 &= -2.9 \cdot 10^{-9} [J] \end{aligned} \quad (4)$$

where:  $Amp$  – the amplitude of sinusoidal excitation signal,  $F_0$  – bias shifting of sinusoidal excitation signal

Inverting the Lennard-Jones function having the selected parameters from (4), an output signal was determined. Both signals are presented on Fig. 5.

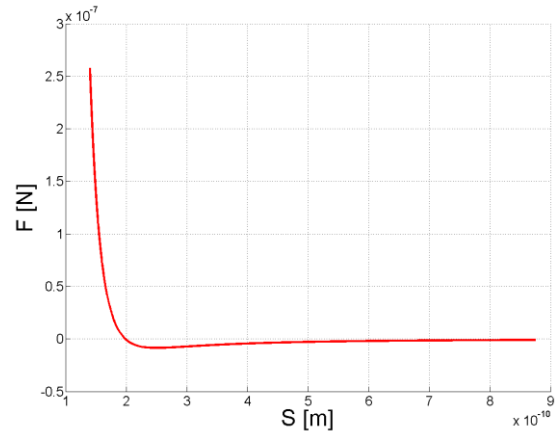


Fig. 3. Modeled Leonard-Jones force function

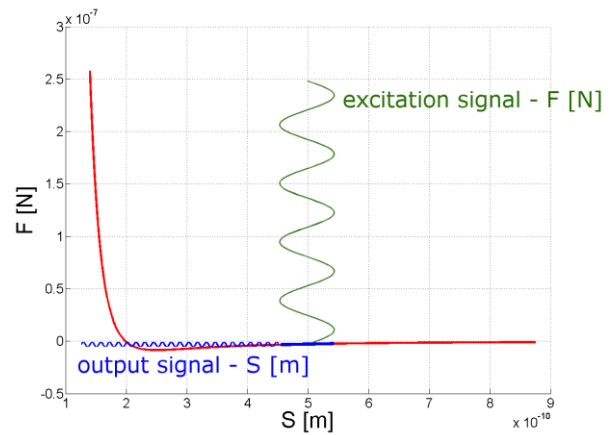


Fig. 4. Modeled Leonard-Jones force function with marked excitation and output signals

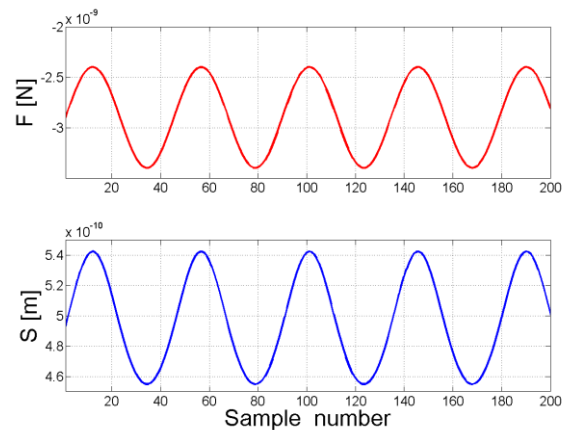


Fig. 5. Stimulation and output signal

Next, after ordering the samples, it is possible to draw the chosen range of non-contact mode. Function  $F(s)$  is presented on Fig. 6. Next, a simple matrix calculations allow getting the coefficients of the reconstructed Lennard-Jones function and described by (5).

In the calculation (5), the  $A$  matrix and stimulating signal  $F$  (with the selected parameters from (4)) are used

to calculate the constant coefficients of Lennard-Jones function ( $c$ ). The variable  $s_2$  is a vector, which contains distance values for which we want to restore the Lennard-Jones function. After multiplying the vector  $s_2$  and the coefficients' matrix  $c$ , we obtained reconstituted the Lennard-Jones function  $F_2$  (Fig. 7).

$$A = \begin{bmatrix} \frac{1}{s^2} & \frac{1}{s^8} \end{bmatrix}$$

$$C = \frac{(A' \cdot A)}{A' \cdot F}$$

$$s_2 = \left[ 0.14 \cdot 10^{-9} \quad 0.14001 \cdot 10^{-9} \quad \dots \quad 0.85 \cdot 10^{-9} \right] \quad (5)$$

$$A_2 = \begin{bmatrix} \frac{1}{s_2^2} & \frac{1}{s_2^8} \end{bmatrix}$$

$$F_2 = A_2 \cdot c$$

where:  $A$  – matrix of the reversed distance powered to 2 or 8 respectively,  $C$  – matrix of the Lennard-Jones function coefficients,  $F$  – excitation signal,  $s_2$  – vector of distance values for restoring the Lennard-Jones function,  $A_2$  – matrix of final recessed distance powered to 2 or 8 respectively,  $F_2$  – vector of the Lennard-Jones function for range  $s_2$

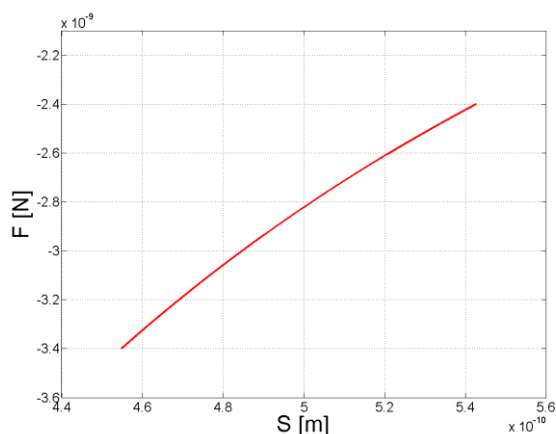


Fig. 6. The simulated fragment of the Lennard-Jones function at non-contact mode

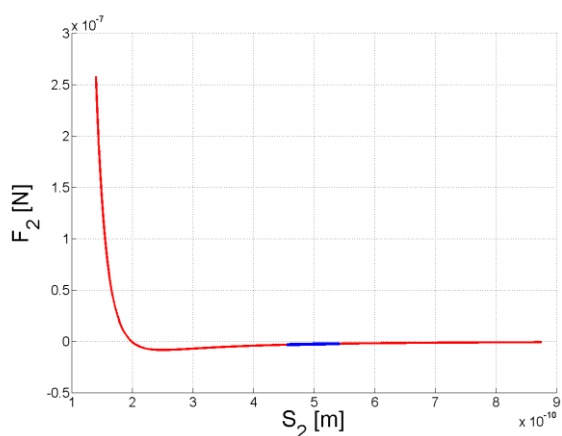


Fig. 7. The reconstructed Lennard-Jones function by simulating signals of cantilever excitation and its vibrations; the bold fragment correspond to the reconstructed fragment

It is possible to extract information about the Lennard-Jones function parameters by analyzing dependence between the stimulating signal and the answer signal (vibrations of the cantilever). The presented results (Fig. 6, Fig. 7) of the prepared simulations confirmed such ability.

### 3. MEASUREMENTS

Measurements were made using a sample of quartz surface. The AFM device collects data of a surface of resolution 256 x 256 pixels. The device records three channels: excitation harmonic signal, output signal of the cantilever vibrations and signal of synchronization. The tip moves between the consecutive pixels and collect data at high level of the synchronization signal. This procedure is repeated for the each row of the picture. Next, the tip returns to begin scanning of the next row (Fig. 8). Each row comprises 256 pixels and vibrations of the cantilever have to be analyzed when the synchronization signal is in high state (Fig. 8). The detailed graph of all three recorded channels presents Fig. 10 ( $Syn$  - synchronizing channel,  $F_V$  - excitation channel,  $S_V$  - vibrations of the tip). The excitation ( $F_V$ ) and vibrations of the tip ( $S_V$ ) signals are measured in volts, but they are proportional to the force acting on atoms ( $F_V$ ) and the distance between them ( $S_V$ ). Both of dependences are linear. After selecting the appropriate pieces of the recorded waveforms, we can draw the fragment of the  $F_V(S_V)$  function (Fig. 10, grey points) for all the measured pixels. The results exhibit some random component due to interferences present within the AFM device. The fragment of the investigated Lennard-Jones function is obtained when the data are averaged over the whole available pixels set (Fig. 10, bold points).

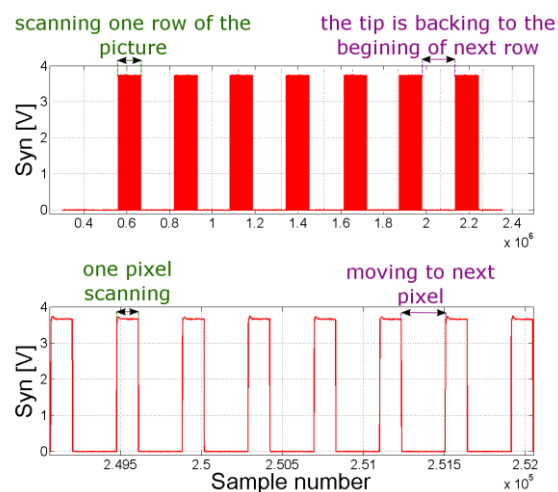


Fig. 8. The synchronization peaks packages of the recorded AFM signals

The Lennard-Jones function was approximated (Fig. 11) by fitting its fragment (Fig. 10) identified by the averaged set, characteristic  $F(s)$  function was determined (Fig. 11).

At this stage of research the measurements results were not scaled (recorded voltage values) into force and distance values due to lack of necessary data. The considered measurements results of voltage values are linearly dependent with force and distance values and therefore all the presented considerations are valid

without application of the mentioned scaling. The similar assumption was taken elsewhere [6] when the normalized differences in the Lennard-Jones function enabled identification of the single atom.

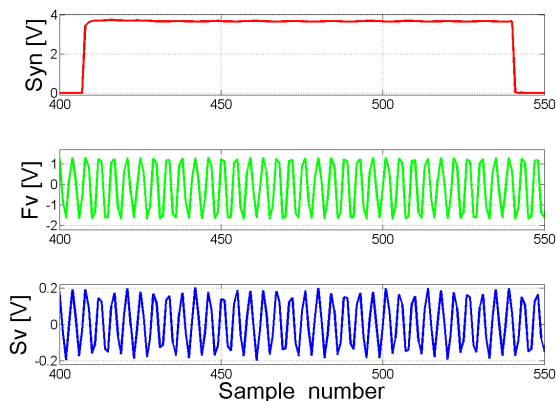


Fig. 9. The zoomed three channels of the recorded AFM signals: synchronous signal ( $S_{yn}$ ), excitation signal ( $F_v$ ), signal of the vibrating tip ( $S_v$ )

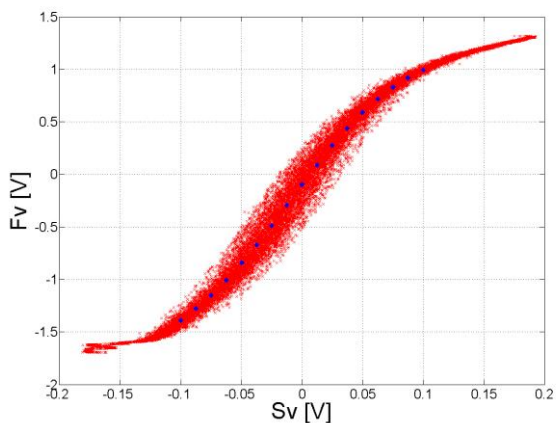


Fig. 10. The identified dependence between the excitation signal  $F_v$  versus the measured distance  $S_v$  and its averaged values (black dots) within the measured data

#### 4. CONCLUSIONS

The presented results describe theoretical considerations how to determine the parameters of Lennard-Jones function by the AFM microscope. The exemplary measured data of the quartz layer were applied to confirm a correctness of the proposed method. This study determined rightly a type of the tested layer.

### SYMULACJA I POMIARY W IDENTYFIKACJI SUBSTANCJI ZA POMOCĄ AFM

**Słowa kluczowe:** mikroskop sił atomowych, identyfikacja substancji, funkcja Leonarda-Jonesa

W związku z rozwojem nanotechnologii, znacząco wzrosła potrzeba badań mikroskopijnych obiektów. Do takich celów służy mikroskop sił atomowych (AFM), który umożliwia badania topografii próbki oraz dostarcza informacji o jej składzie chemicznym. W ciągu ostatnich dwóch dekad liczba możliwych zastosowań AFM znacznie wzrosła. Mikroskop AFM bada siły oddziałujące między atomami igły skanującej a powierzchnią próbki. Siły te opisuje funkcja Lennard-Jonesa. W pracy przedstawiono teoretyczne podstawy działania mikroskopu sił atomowych oraz rejestrowane sygnały, służące do identyfikacji badanej substancji. Przykładowe badania wykonano na próbce kwarcu. Przyjęty sposób analizy danych pokazuje, jak uzyskać parametry funkcji Lennard-Jonesa, charakterystycznych dla badanej próbki.

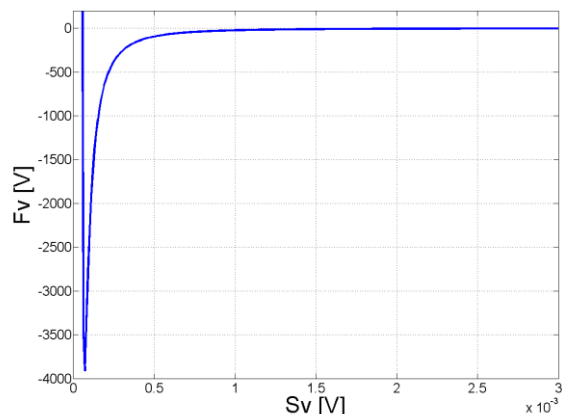


Fig. 11. The approximated Lennard-Jones function by using the measured data for the quartz layer

#### 5. REFERENCES

1. Hasse L., Šikula J., Smulko J., Spiralski L., Szewczyk A.: System do badań nieniszczących warystorów metodą spektroskopii ultradźwiękowej, Zeszyty Naukowe Wydziału Elektrotechniki i Automatyki Politechniki Gdańskiej Nr 25/2008, Gdańsk 2008, s. 61-66, ISSN 1425-5766
2. Binnig G., Quate C. F., Gerber Ch.: Atomic Force Microscope, Physical Review Letters, Vol. 56, Marzec 1986, s. 930-934
3. Blanchard Ch. R.: Atomic Force Microscope, The Chemical Educator, T. 1, Nr 5, Springer-Verlag, New York 1996, s. 1-8, ISSN 1430-4171
4. Dror S.: Exploring Scanning Probe Microscopy with MATHEMATICA, Wiley-Vch, Weinheim 2007, ISBN 978-3-527-40617-3
5. Das S., Sreeram P. A., Raychaudhuri A. K., Phanindra Sai T., Brar L. K.: Non-Contact Dynamic Mode Atomic Force Microscope: Effects of nonlinear atomic forces, Emerging Technologies - Nanoelectronics, 2006 IEEE Conference on, s. 458-462, ISBN: 0-7803-9357-0
6. Sugimoto Y., Pou P., Abe M., Jelinek P., Pérez R., Morita S., Custance Ó.: Chemical identification of individual surface atoms by atomic force microscopy, Nature, Vol. 446, Nr. 7131, Londyn 2007, s. 64-67, ISSN: 0028-0836